IEEE Access
Multidisciplinary | Rapid Review | Open Access Journal

Received April 14, 2021, accepted April 30, 2021, date of publication May 5, 2021, date of current version May 13, 2021.

Digital Object Identifier 10.1109/ACCESS.2021.3077728

Internet of Things in the Railway Domain: Edge Sensing System Based on Solid-State LIDAR and Fuzzy Clustering for Virtual Coupling

GABRIEL MUJICA, (Member, IEEE), JAVIER HENCHE, AND JORGE PORTILLA, (Senior Member, IEEE)
Centro de Electrónica Industrial, Universidad Politécnica de Madrid, 28006 Madrid, Spain

Corresponding author: Gabriel Mujica (gabriel.mujica@upm.es)

This work was supported by the SCOTT project from the Electronic Component Systems for European Leadership Joint Undertaking under Grant 737422.

ABSTRACT Recent advances in wireless communication, sensing and processing technologies are fostering novel research and innovation opportunities in areas such as Industry 4.0, Smart Cities and Intelligent Transportation Systems. In particular, the railway domain is envisioned to have important breakthroughs in terms of cost-efficiency, self-management, and reliability in the operation of the rolling stocks and infrastructures. Some of these key objectives are been addressed by the concept of Railway Virtual Coupling, which is a promising solution where the capacity of the tracks is highly improved by means of reducing the distance between adjacent trains, and the physical connection between train's compositions, through accurate Vehicle-to-Vehicle communication systems. In this work a new approach towards supporting the information dynamically exchanged by the trains is proposed, with the design and implementation of a Solid-State LIDAR based sensing system to provide an accurate, robust and low-latency on-board distance detection system between trains. The combination of a long-range distance sensor, an Internet of Things (IoT) edge hardware platform and a fuzzy clustering approach for distance detection of the object of interest allows obtaining very accurate results to support the virtual coupling maneuvers. The system implementation has been tested in a real railway scenario, where several coupling and distance detection maneuvers have been performed to verify the operation of the proposed system in an actual application context. This represents one of the first dedicated distance detection tests of this kind under real dynamic conditions documented in the literature towards railway virtual coupling.

INDEX TERMS Edge nodes, Internet of Things, LIDAR sensing, railway application, wireless sensor networks.

I. INTRODUCTION

The continuous advances in wireless communication, sensing and processing technologies are opening up new research and innovation opportunities towards cost-efficiency, sustainability, self-management and reliability in areas such as Smart Cities, Industry 4.0, and Intelligent Transportation Systems. Important European initiatives [1], [2] are bringing technological solutions for improving safety and security, capacity, resource efficiency and infrastructure operation in the Railway domain. In particular, the optimization of the rail tracks is one of the key challenges to be faced in today's and future research projects, since nowadays the use of the infrastructures and circulation of different nearby trains is limited by the minimum safety distance handled by the control and protection systems.

For instance, in standard lines these distances are managed by Train Detection Systems (TDS), where each TDS has a minimum length of 600 m. The Traffic Management Systems (TMS) shall control that a minimum of X TDS (which depends on the European regulations [3]) must be kept to assure a safety breaking distance. This ultimately imposes the capacity and the limitation of the number of trains on track. Moreover, the issue of multiple train compositions that can

The associate editor coordinating the review of this manuscript and approving it for publication was Liang-Bi Chen.

be reconfigured during the whole journey (since some parts of the train have different destinations) is traditionally tackled by carrying out long stops and splitting actions, which leads to spend resources for performing such operations.

These challenges are being faced by what is known as Railway Virtual Coupling, in which a more Train-Centric approach [4], [5] allows performing very precise self-monitoring and detections between adjacent trains, in order to carry out automatic coupling/uncoupling manoeuvres. This will eventually allow increasing the capacity and occupancy of the track, since the distance between trains can be reduced within safety and accurate margins, and with operational cost efficiency. Moreover, physical coupling manoeuvres between train's compositions are minimized, reducing the time, resources and cost associated to such operations. Moving from dedicated infrastructure systems towards a decentralized and distributed approach where a direct data exchange between trains plays a important role, the Vehicle-to-Vehicle (V2V) communications are the primary strategies to carry out the virtual coupling implementation, where low-latency highly-reliable radio links are fundamental to manage time-critical events.

The Secure, COnnected Trustable Things (SCOTT) Ecsel JU European project addresses this concept, by the design and implementation of a complete Smart Train Composition Coupling architecture, and with a particular focus on the integration of Internet of Things (IoT) technologies [6]. Unlike other works in which the virtual coupling system only relies on the radio links between trains [7], the SCOTT project, and in particular the railway domain use case, also adds another means of direct distance measurement with the inclusion of Wireless Sensor Networks (WSN) in each train, whose information can be exchanged in a distributed and real-time manner between them. This includes data related to the train composition, mass, weight and length properties, location, among others. Combining the sensing capabilities of the trains with the V2V communication links, the coupled trains will be able to perform moving manoeuvres in a safety manner. Based on this rationale, in this article a distance sensing system for railway virtual coupling and its integration within the Smart Train Composition Coupling is addressed. The main target is to integrate a reliable and precise distance measurement system with an IoT edge platform to accurately provide the distance detection between virtually coupled trains.

Much effort has been dedicated in the state of the art to develop object detection for collision avoidance systems, particularly in terms of precisely distinguishing between several types of possible collision objects in the field of view and classify them, considering shapes, size of the type of object, and location information, especially for unexpected objects on the railway tracks, or in autonomous vehicles to avoid road accidents and crashing damages. For instance, there are works that classify the possible types of collisions to implement specific feature extraction techniques and algorithms to trigger warning alarms, such as in [8]. However, in this work the main objective is rather detect the presence of adjacent trains and precisely determine the distance from one train to another, so both the accuracy and range of the distance measurement are the fundamental elements to be considered for the virtual coupling maneuvers and the operation of the V2V system. In this way, while different works in the literature are centered in how accurate the detection of the type of the object is performed, most of them do not consider the dynamic conditions, composition, speed and distance required for virtually coupled moving trains, as in case of the different maneuvers and actual V2V coupling operations studied in the present work.

There are important challenges and requirements to deal with when considering the distance sensing between trains, in order to provide a feasible and accurate value to feed the virtual coupling system. In particular, a long range detection, a high resolution in the measurement, and a short time response are key to cope with safety requirements. These constraints are to be combined with reliability, low noise in the measurement, and robustness. As a result, in this work a very promising technology is explored: the Solid-State LIDAR (Light Detection and Ranging, or also known as Laser Imaging Detection and Ranging) sensing, which provides a combination of accurate measurement results and high resolution with robustness, since no mechanical moving parts are integrated in the sensor as in case of traditional LIDARs. This is a very critical aspect in the railway domain, since vibrations and train movements are to be considered for minimizing on-board system failures.

While rotational LIDARs can provide a 360° view to perform object detection tasks, the Solid-state LIDAR is limited to a narrow field of view focusing on a target region, to detect with very high precision the distance to an object of interest from short to long ranges, and with considerably lower costs than the former ones. The information provided by the LIDAR sensor is fully exploited to perform the detection of the object of interest by using a fuzzy-clustering based approach, which is one of the primary objectives of the work. The main contributions of this work are summarized as follows:

- Implementation of a long-range highly accurate distance sensing system for train virtual coupling, based on the integration of IoT edge technologies and Solid-state based LIDAR sensing in the railway domain.
- Design and embedded integration of fuzzy clustering strategies to further process and tune the distance detection to the object of interest, which is the adjacent coupled trains, based on the information provided by the LIDAR sensor. The proposed adaptation of FCM (Fuzzy C-Means) algorithms allows providing more adjusted distance detection results of the objects within the field of view of the sensor.
- Based on the aforementioned contributions, the experimentation and proof of concept of the proposed system has been carried out within a real railway scenario with different train coupling and moving manoeuvres, to verify the functionalities provided by the distance sensing

platform with actual trains, and in dynamic operational conditions. This is a very valuable and one of the first distance detection tests of this kind documented in the literature towards railway virtual coupling.

The rest of the article is organized as follows: Section II presents an overview of the main trends in the state of the art related to LIDAR systems, object detection and clustering algorithms, and how these technologies are employed in different application domains. Section III is devoted to detail the proposed solid-state LIDAR based distance sensing system, and the description of the specific hardware elements integrated in its design and implementation. The implemented embedded fuzzy clustering algorithms for distance detection of the objects of interest within the field of view is also presented in this section. A set of experimental tests considering a first characterization and then a verification of the implemented system in a real railway domain use case is reported in section IV. Finally, conclusions and future work are highlighted in Section V.

II. RELATED WORK

A. OVERVIEW OF LIDAR SYSTEMS

One of the areas in which LIDAR sensors are being widely used is the automotive sector, where they can offer information about the obstacles of the surrounded scenario. This type of sensors can be found in all types of vehicles, from road vehicles [9]–[11] such as cars, trucks or buses, to autonomous land vehicles [12].

All the previous cases share the same particular characteristic: the LIDAR is mounted on a mobile platform. In situations in which it is intended to perform a detection of moving objects, commonly known as DATMO (Detection And Tracking of Moving Objects), it may imply several challenges. To be able to distinguish and classify the objects, the fact that the sensor is in motion increases the complexity, since objects that are actually static, and might not be of interest, may appear moving relatively to the sensor.

Vehicle-mounted LIDARs can also be used to map a scenario that is a priori unknown. In addition to mapping, if the objective of the vehicle is also to position itself for navigation through the target environment, these types of problems are often referred to as SLAM (Simultaneous Localization And Mapping). A type of vehicles on which the sensor is often mounted to perform the SLAM are called Unmanned Ground Vehicles (UGV), as in [13], [14] where the environment explored in these cases is the interiors of buildings.

LIDAR-based systems can also be found in aerial vehicles to scan the terrain, vegetation, or any other objective, from a top perspective. In [15] the height of forest vegetation is obtained exclusively from a LIDAR, mounted on an aircraft, to assess the state of the target area. In [16] a low cost system is proposed, in which other types of sensors and cameras are mounted on an Unmanned Aerial Vehicle (UAV) in addition to a LIDAR, to obtain the maximum information available in different situations such as the study of roads, trees and forests, and snowy areas. LIDAR sensors are also employed in other areas besides vehicles. Sometimes the scanning of objects and scenarios is not done on a mobile platform, but by a group of people, taking samples of the points of interest. This is the case of [17], where an operator is able to take the measurements obtained from a LIDAR to get a three-dimensional map of a cave. Or as in [18], where the system gets characteristics of two types of forests from different static landmarks on land, by using the sensors.

B. OVERVIEW OF OBJECT DETECTION SYSTEMS AND ALGORITHMS

One of the purposes of using LIDAR sensors is to distinguish objects from a set of distance measurement points (known as point cloud). Artificial vision systems capable of distinguishing patterns and shapes from among all available pixels in an image have been developed in recent decades. In addition to the image of a camera (which provides a flat projection of the field of view), the information provided by a LIDAR sensor can be used to offer distance measurements in the joint field of view of the camera and the sensor. Several techniques used in the detection and tracking of objects from video images are compiled in [19]. To track an object in an image, it must first be identified, either by its shape, or by its movement (or absence thereof). Once the object has been identified and characterized, the monitoring is carried out through the information of past moments, with which the trajectory of the object can be obtained until the present instant.

The existing methods for the detection of elements can be divided into two groups: A first group, based on models (model-based) in which the detection of objects relies on predefined characteristics already known from the body/object. These characteristics are usually related to the shape or size of the body that is being detected. The second group, by contrast, lacks an object model (model-free) and seeks to distinguish it from the rest of the environment using other characteristics, mainly movement, and discarding objects that are static. In this second group, the shape or size of the object is not restricted, but any element that is not moving is ignored.

Within the first group (model-based), the work proposed in [20] is able to detect people through a model obtained by means of a self-learning algorithm (Adaptive Boosting), which extracts the main characteristics of the readings that the LIDAR carries out of the legs of people in different circumstances. Once a set of measurement points is associated with a pair of legs, the position of that person is monitored by a tracking algorithm. Another example is that of [21], where cars are modeled as rectangles, and the set of typical measurements that are obtained from a LIDAR in the defined geometric form are sought. For the simultaneous detection and tracking of the object, an MCMC (Markov Chain Monte Carlo) algorithm is used.

In the second group, there are solutions such as in [10], [11], [22], [23], where there is no restriction on the type of objects that can be detected in the set of measurements. In [11], from a set of segments (groups of measurements close to each other) special characteristics are extracted based

on their form, which are used to locate the segment and detect its movement. Then, it will become an object that will be subsequently monitored. In [22], a process similar to the previous one is followed, where special characteristics that are independent of the perspective obtained (corners) are sought, and the set of points with such characteristics is monitored. In this case, the environments are restricted to freight ports. In [10] and [23], the segments are compared over time, and they are classified as static, which would be part of the environment, or in motion, so that they would become an object of interest.

In both groups a pre-processing is performed prior to the selection of objects of interest, namely segmentation. This segmentation consists in grouping the points detected by proximity in sets of points close to each other. In [11], if a point is at a distance less than a predetermined threshold from the set, then that measurement point is included within it. In [22] a similar procedure is followed based on the distance between points. However, instead of defining a constant threshold, the threshold is determined based on the distance of the measuring points to the sensor. This prevents over-segmentation (many groups with few points) on distances far away from the sensor.

One of the challenges that segmentation algorithms must manage is the occlusion problem. When a small obstacle appears in the line of sight between the LIDAR and the object that is being detected, it can segment the set of measurements assigned to that object, and thus divide it into two or more groups, losing its real position.

There are also works in the state of the art regarding object detection for autonomous driving and railway collision avoidance systems, mainly using image processing and feature extraction techniques from cameras, and also point-cloud projection methods from LIDAR sensors [24]. Depending on the type of data processing and object detection strategy they use, higher computational resources are needed to cope with the complexity and requirements of the training stage and the runtime execution of the algorithms. In [8] authors use feature extraction mechanisms from a camera installed in the train to distinguish between different types of objects in the field of view (in particular pedestrians in the track). In [25] different direct and indirect collision scenarios are taken into account to avoid accidents particularly with animals. Authors use computer vision strategies with a camera and they study the possibility of calculating the distance to the object of interest by correlating the depth of the object in pixels once it is detected, for short-range distances (20 meters maximum).

However, the use of cameras might reduce drastically the accuracy in case of difficult weather and light conditions, or for detecting long-range distance objects, which can compromise the safety requirements depending on the target application context.

C. FUZZY CLUSTERING

Fuzzy Logic emerges as an alternative to binary logic [26], in which the variables instead of being limited exclusively to values of zero or one, can have an intermediate value between binary limits. As seen in the previous subsection, for the detection of objects the segmentation of spatial information is widely used, either from video information or obtained with LIDAR sensors. With segmentation, a series of measurements or pixels are grouped into segments based on distance, brightness, or other variables. In this way, a series of measurements or pixels is grouped in a binary and exclusive way, and therefore, each of them can only belong entirely to one segment. It is in this technique where it is possible to apply fuzzy logic, so that the division between segments is not drastic.

To achieve this, FCM algorithms (Fuzzy C-Means Clustering) [27], [28] can be used. This type of algorithms allows blurring the degree of belonging of each element to a cluster, given some segments or clusters already defined. The belonging degrees are distributed among the rest of the clusters, depending on the distance of the element to the centroid of each segment. Based on that, in the borders between segments the degrees of belonging of the elements in those borders are divided between the clusters present in those limits, especially in cases in which the segments or clusters are close.

This algorithm can be used to make fuzzy clusters of any multi-variable data type. In particular, this type of technique has been mostly used for image analysis, such as in [29], [30], where images of the brain and the skull obtained from magnetic resonance imaging are employed to perform image segmentation, and thus facilitate health diagnosis. Moreover, FCM has been recently used in diverse areas such as spectrum sensing, human genome analysis, and image segmentation in geometric modelling [31]–[33].

III. PROPOSED SYSTEM

The core of the vehicle-to-vehicle distance detection system for railway virtual coupling is mainly composed of an Internet of Things Edge processing platform and a solid-state LIDAR sensor. While the later is in charge of taking the distance measurements within its field of view, the first one will process the LIDAR segments to finally obtain the distance from the sensor to the object of interest, in this case from one train to the other. Fig. 1 depicts a schematic view of the proposed system, where the main hardware and software elements are highlighted.

A. LIDAR SENSOR

The LIDAR used for the proposed system is the Leddar Vu8 from LedarTech [34], which is a solid-state based small-size LIDAR technology, so no moving parts for mechanical rotation of the beams are used. The model used in this work has a configuration of a narrow field of view (FoV) of 20° in a plane. The maximum detection distance of the LIDAR is 185 m. Within the field of view, there are eight measurement segments, from which distance and amplitude data is obtained for each one of them. Table 1 summarizes the main characteristics of this LIDAR.

Unlike 3D rotational LIDARs, the amount of data provided by this sensor is certainly limited, although the later has a

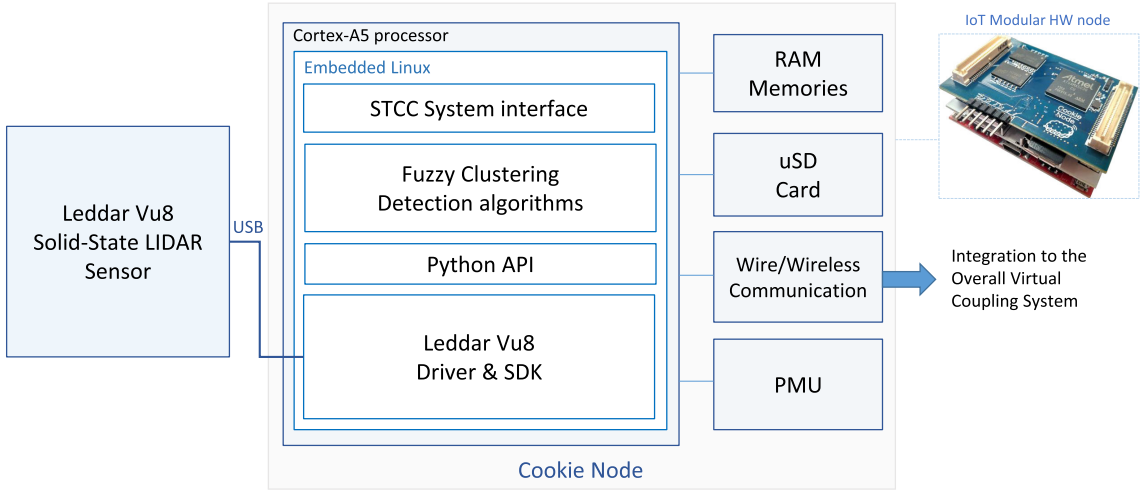

FIGURE 1. General architecture of the proposed system, with the integration of the Solid-State LIDAR sensor and the IoT edge platform.

TABLE 1. Main characteristics of the Solid-State LIDAR sensor.

Attribute	Specification value
Number of segments	8
Field of View (FoV)	20º
Vertical FoV	3º
Dimensions	70.0 mm x 35.9 mm x 71.2 mm
Wavelength	905 nm
Distance accuracy	5 cm
Interface to the Host	USB
Power consumption	2 W
Weight	110 g
Ocular safety	IEC 60825-1:2014 Class 1 laser
Operating temperature	-40 °C to +85 °C

considerable lower cost (approximately an order of magnitude). After the pre-processing performed on the sensor, the available data correspond to the segments. Therefore, there are only eight distance measurements, each corresponding to a field of view of one eighth of the 20 degrees. Comparing the data provided by this sensor with others in the literature, which rarely have less than 100 measurement points, this LIDAR has a low resolution. Nevertheless, the main benefit comes from a precise long-distance measurement in combination with the processing of the FoV segments to detect the presence of the object of interest, which is the aim of the proposed system.

Another difference with other sensors is that the measurements do not correspond to a point, but to a fraction of the FoV. Therefore, each segment covers its own FoV, and the corresponding measurement takes into account all surfaces within it. This means that if two surfaces share a segment's FoV, the distance measured by that segment will be an intermediate value of the two distances from the sensor to the surfaces. The contribution to the final distance from each surface will be proportional to its degree of occupation of the segment's FoV.

B. IoT EDGE PLATFORM

The proposed system relies on the use of an IoT Edge node for Wireless Sensor Networks, called Cookies [35], [36]. It is an IoT hardware platform developed at the Center of Industrial Electronics (CEI-UPM) where the concept of modularity, flexibility and reliability is maximized. Its main feature is the capability of modifying the hardware setup in a modular way, integrating and reusing different layers that perform different functions (namely processing, communication, sensing and power supply layers). Fig. 1 also shows a general view of the Cookie node, where the modular hardware layers can be seen. Each layer can be adapted and redesigned to the particular characteristics and requirements of the target application, that is, from ultra-low power processing layers to high performance computing capabilities on the Edge, or the integration of a variety of different sensor and communication technologies.

The version of the processing layer to be used in this work provides a trade-off solution between Edge embedded computing and power consumption. It is based on an ARM Cortex-A5 processor, the ATSAMA5D36 from Microchip (formerly Atmel) [37], and 256 MB of RAM with a clock speed of 536 MHz, in addition to having USB, UART, SPI, I2C connection interfaces for external connections with other hardware components, such as in case of the Leddar Vu8. It runs a embedded Linux Operating System (Debian 9 stretch), upon which the LIDAR control API and the developed algorithms are implemented and executed.

C. SENSING PROCESSING ALGORITHMS

The main objective of the developed algorithms is to obtain the distance of the object of interest closer to the sensor, which corresponds to the distance to the nearby on-track train. It also seeks to take advantage of all the information provided by the sensor to know and characterize as much as possible the environment under detection.

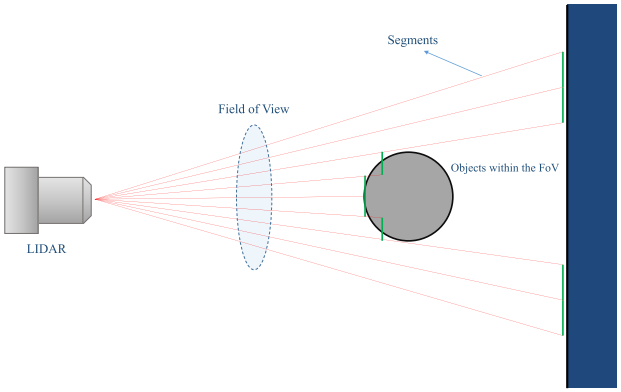

FIGURE 2. Field of View (FoV) of the solid-state LIDAR, with the representation of the 8 segments, and two different objects within the FoV.

First, a segmentation of the field of view will be performed to group the eight measurements according to the distance between them. From now on, instead of calling this process segmentation, in this work it will be called ''clustering'', to make a distinction between the segments provided by the Leddar Vu8 and the processing performed on the Edge platform. After clustering, the nearest cluster can be designated as the object of interest, and its distance and relative speed to the LIDAR can be obtained.

1) INITIAL CLUSTERING

As explained before, the Leddar Vu8 sensor has an eight segment resolution for its 20 degree FoV. Fig. 2 shows a representation of how the FoV is divided into eight segments. Each segment covers approximately 2.5° of the FoV. The distance will be taken for each segment that reaches the object within the FoV (in this case the wall and the middle object). The objective of the clustering algorithm is to group the given segments, considering that each group corresponds to a detected object, being able to distinguish between several objects in the LIDAR's FoV. In case of a single surface in the FoV (for instance the wall without the object in the middle) the algorithm should join all segments into a single cluster.

Now consider that an additional object would be introduced in the LIDAR detection field, as shown in Fig. 2. In this case more than a single cluster shall be detected. By having a new object in the field of view, the algorithm must be able to group all the segments that detect it into one cluster, and the rest of the segments will be divided into other two clusters, the two corresponding to the object on the background. In order to group the segments provided by the sensor, the distance between each segment will be first acquired. Determining this distance is simple to calculate, making the difference between the distance vectors from the segment to the sensor, and obtaining the module, as can be seen in Fig. 3. It will be the result of subtracting both distance vectors from the pair of segments. The module of the vector obtained in this operation will be that distance.

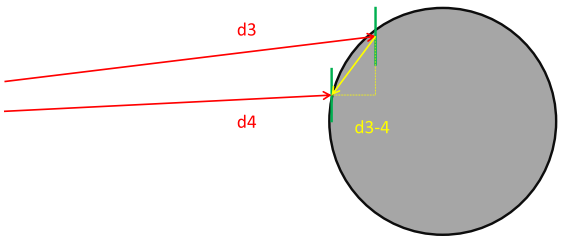

FIGURE 3. Illustration of the distance calculation between segments.

If the distance between segments is lower than a certain threshold, those segments become part of a group. In this way, the distance between all adjacent segments is compared to each other. If the segments are close to their adjacent ones, they will belong to the same cluster. Otherwise, they will become part of another cluster of segments. Up to eight different clusters can be created, in case each segment is sufficiently separated from the two adjacent ones at each side.

The threshold for considering that two segments are close enough to each other will be calculated based on the distance at which the sensor segments are. The greater this distance is, the greater the threshold will be. Since the segments keep a constant angle of 2.5° to each other, as the distance they are from the sensor grows, the minimum distance between them will also grow. Taking into account this, the threshold will be obtained from the theoretical minimum distance between two segments depending on the distance to the sensor. This theoretical minimum separation is computed by applying trigonometry calculation.

Obviously, the threshold will have to be slightly larger than the minimum separation in order to group segments. For this reason, the minimum separation is multiplied by a factor that is configurable. The larger this factor is, the lower the threshold will be, and therefore, the clusters may include more separate segments between them. Therefore, the proper adjustment of this factor is essential, so that neither segments that correspond to different objects are grouped, nor segments belonging to the same object are divided into different groups. Because the threshold depends on the distance of each segment to the LIDAR, it must be calculated for each of the eight segments available.

Taking into account this procedure, the clustering algorithm must first obtain the separations between each pair of segments, then calculate and verify the threshold boundaries for each pair of segments, and finally group each segment into a cluster depending on whether the distance between that segment and its adjacent ones are below the threshold. Fig. 4 shows a diagram that depicts the procedure performed by the algorithm.

For the example of Fig. 2, the result obtained would be three clusters, the two ends corresponding to the background wall, and the central cluster that belongs to the object of interest. Fig. 5 illustrates the result applying the described algorithm.

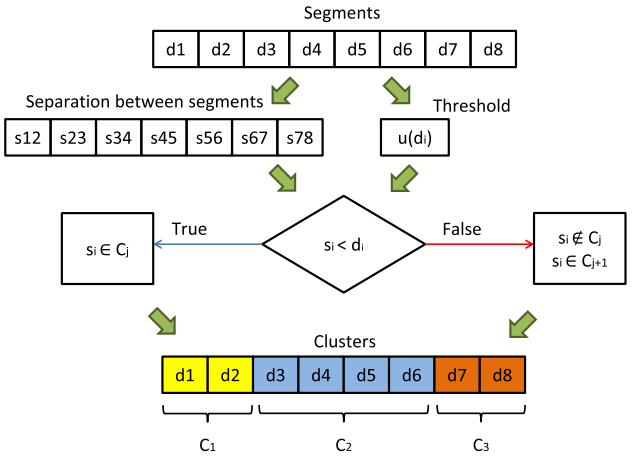

FIGURE 4. Schematic representation of the clustering algorithm.

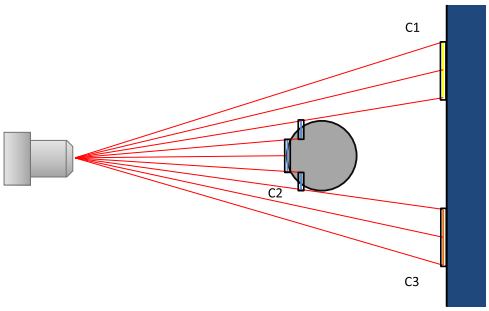

FIGURE 5. Illustration of the clustering results for the example of two different objects in the FoV.

A possible limitation is that if a small object is interposed between a larger one and the LIDAR, the larger object will have to be divided into two clusters, so it cannot be assumed that a cluster belongs unambiguously to an object or surface, as happens with the background wall of the figure. In this case, it might be considered as a single object based on the distance to the object, although it could happen that two different objects are at the same distance from the sensor. In case of the closest cluster to the sensor, it can be assumed that it is a single object or, at least, a set of objects very close to each other, which can be considered as the same entity.

As explained in the previous section, another phenomenon that might also happen is that in the same segment two surfaces coexist at two considerably different distances (as represented in Fig. 6). Depending on the threshold value, it may occur that a separate cluster is created just for that intermediate segment. Because the intention of the clustering algorithm is to generate a cluster for each present object, having an independent cluster that does not belong to any of the two existing objects is a problem that must be managed. This type of results are solved with the solution proposed in the following section, which tries to provide a closer outcome to the real existing objects within the FoV of the LIDAR sensor.

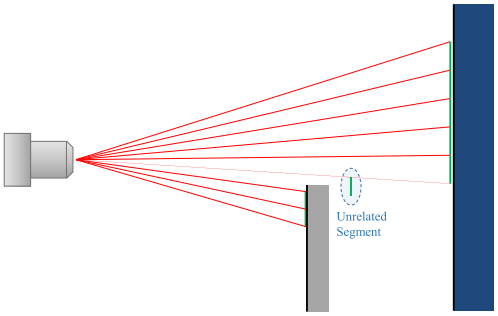

FIGURE 6. Illustration of the unrelated segment phenomenon.

2) FUZZY CLUSTERING

With the initial clustering method it is possible to divide the sensing measurements into different groups, being able to distinguish objects according to the distance. However, each measurement can only belong to one of all possible clusters that have been obtained. In other words, for each cluster, the measurement may or may not belong to it, which is a purely binary distinction.

By using fuzzy logic, such a differentiation may not be so radical. Its utilization can be very useful especially in cases where the belonging of a measurement to a cluster is determined even if it exceeds a threshold by a very small margin. In these borderline cases, membership to one cluster or another may become arbitrary depending on the chosen threshold. When the distance between two measurements that actually corresponds to the same object is slightly greater than the threshold considered to group them, there would be two measurements that should be grouped together when detecting the same body, but the clustering algorithm would separate them into two different clusters as the distance between them is greater than the threshold.

The objective of the ''fuzzification'' of the clusters is to ensure that the membership of the measurements to each cluster is not binary. That is, a distance measurement can have a degree of belonging to several clusters at the same time. In this way, the error due to a wrong assignment of a measurement to a cluster to which it should not belong to is considerably minimized. At the same time, this process will be able to ensure that the measurements that do correspond to that of an object in the measurement space have a clear belonging degree to the cluster corresponding to that object.

To achieve this optimization goal, in this work the FCM (Fuzzy C-means clustering) algorithm is used. It employs the results obtained in the previous clustering process as the initial data, according to which each measurement will have a degree of belonging equal to 1 for the cluster assigned to it, and 0 for the rest of existing clusters. In this way, one or more arrays of belonging, that is, a membership matrix initialized by the clustering algorithm will be available. An example of the membership matrix initialization can be seen in Fig. 7. Each row represents the degree of belonging of the eight measurements from the LIDAR to each cluster obtained by

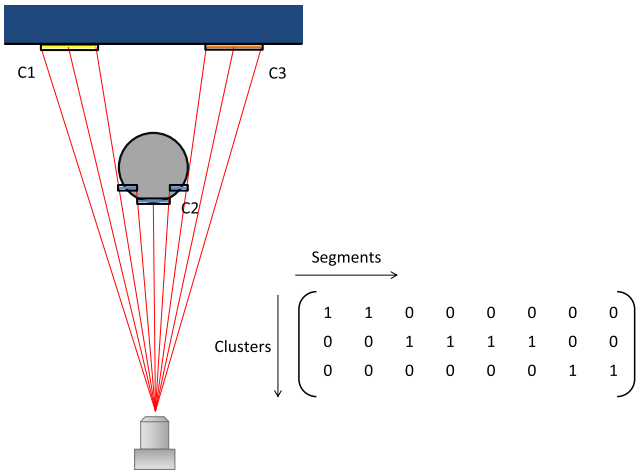

FIGURE 7. Membership matrix relating the LIDAR segments with the clustering detection.

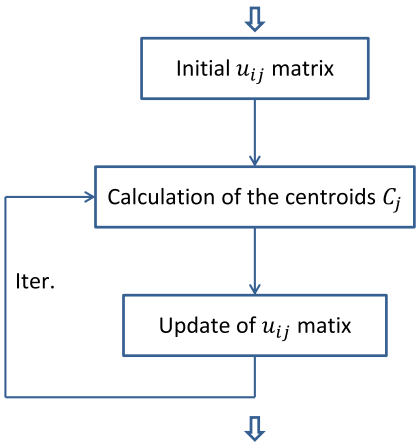

FIGURE 8. General diagram of the runtime fuzzification iteration process.

the algorithm. As it can be seen, the degree of belonging is binary.

With the information generated by the initial clustering process, the centroid position of each cluster will be calculated based on the position of each measurement, as well as its degree of belonging to that cluster, as shown in equation 1, where the degree of belonging is represented by u and the position of the measurement by x.

$$Cj = \frac{\sum_{i=1}^{8} u_{ij} \cdot x_{ij}}{\sum_{i=1}^{8} u_{ij}} \tag{1}$$

Then, the membership matrix will be updated, recalculating for all the measurements their belonging to the initial clusters. This is done through equation 2.

$$Uij = \frac{1}{\sum_{k=1}^{C} \left(\frac{\|x_i - c_j\|}{\|x_i - c_k\|}\right)^{\frac{2}{m-1}}} \tag{2}$$

As shown in this expression, the result of the new membership of the measurement i to the cluster j will be made based on the distances between the position of the measurement i and the rest of the clusters' centroids. The m factor, which should be greater than one, will determine how diffuse the distribution of belonging to each cluster is. The larger m, the more diffuse the belonging will be, that is, they will be more distributed among the clusters, moving away from extreme values such as one or zero.

This process is iterative. Therefore, with the new matrix of belonging, the position of the centroids will be recalculated, and then a new matrix of belonging will be obtained again, reiterating this process as many times as necessary. In Fig. 8 a general diagram of the "fuzzification" algorithm is sown. With each iteration of the process, the variation between the old matrix and the new one will be smaller each time. Therefore, after a number of iterations the fuzzification algorithm will quit the loop. It is certainly possible to calculate this variation, and leave the loop when it is smaller than a determined value. However, to simplify the calculations and give consistency in the processing time of each series of measurements, the number of iterations has been set to be fixed. Consequently, the variation between matrices (the module of the difference between the old and the new one) should not be calculated, and the execution time of this part of the processing will be more similar for different sets of data. Moreover, this avoids that a bad choice of the limit value between the differences causes the process to remain stuck in an infinite loop.

After obtaining the membership matrix, the characteristics of the clusters (size, position) will be calculated so that each measurement has a contribution to the characterization of the cluster proportional to its degree of belonging in the corresponding cluster. Thanks to this algorithm it will be possible that in borderline cases in which the measurement has been included in a cluster by very reduced margins, it has the chance of distributing its information among several adjacent clusters depending on its distance from them. This result will be more faithful to reality.

Taking the previous example of the initialization of the membership matrix, the result of the final membership matrix should have values similar to those shown in Fig. 9. As it can be seen, the matrix of belonging does not vary significantly, since the objects have a considerable separation, and therefore the initial matrix sufficiently conforms with the reality of the FoV.

However, in case the object corresponding to cluster C2 is closer to the wall detected before, it would be possible that initially the measurements of the ends between C2 and the other two clusters could become part of C1 and C3. After the fuzzy clustering, the contribution of these measurements would be distributed among the clusters, as shown in Fig. 10.

Although this algorithm allows solving the problem that arises in this type of cases, the initial clustering algorithm and thus the generation of the initial membership matrix is critical, since it is the one that determines the total number of clusters, and therefore the number of objects detected.

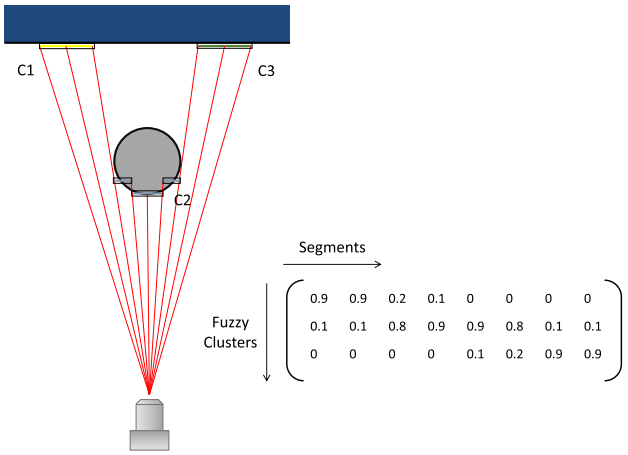

FIGURE 9. Membership matrix relating the LIDAR segments with the fuzzy clustering results.

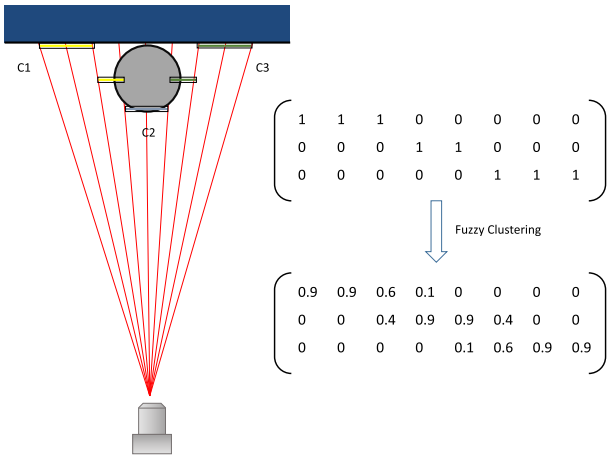

FIGURE 10. Membership matrix relating the LIDAR segments with the cluster detection and fuzzy clustering results, for the example of nearby objects.

Consequently, if there are problems to differentiate objects that are sufficiently separated, the parameters of the algorithm shall be readjusted, since the fuzzy clustering algorithm will not be of great help if the generation of clusters is inaccurate from the start. In cases in which a partial occupation of a segment by two surfaces occurs, the fuzzification algorithm will distribute the ownership of the intermediate segment between the other two clusters, then adjusting the clustering to this particular situation.

It has been considered in this work that the object of interest will be the cluster closest to the LIDAR sensor. This criterion has been mainly chosen because it is the one that offers higher guarantees in terms of safety, since the closest object can be considered as the most potentially dangerous. But also, because the distance of the cluster is the most robust attribute of all available. The object of interest can be also chosen in relation with certain size. The problem with this criterion is that, due to the limited field of view of the LIDAR, sometimes the size cannot be accurately characterized, since there is a possibility that the object only enters the field partially. Also, the problem that arises when a small object is interposed between a larger one, which can cause the larger segments to be divided into several groups. Nevertheless, a correlation of several criteria can be performed to better adapt the algorithm to the detection of the object of interest. The result of this distance detection to the object of interest feeds the Smart Train Composition Coupling system, which ultimately combines this information with the data exchanged by the V2V communication between the coupled trains during the different manoeuvre stages.

TABLE 2. Distance measurement results obtained from the LIDAR segments, for each indoor test.

	Distance measurement from LIDAR segments (meters)							
Test	**1**	**2**	**3**	**4**	**5**	**6**	**7**	**8**
1	2.89	2.21	2.00	2.04	2.08	2.18	2.89	2.96
2	3.12	3.04	2.65	2.50	2.61	2.82	3.00	3.07
3	2.87	2.98	3.00	2.95	2.94	2.34	1.96	1.97

IV. EXPERIMENTAL TESTS

A. PRELIMINARY ANALYSIS

A series of preliminary experiments have been first carried out to test the operation of the overall system implementation and verify that the clustering outcomes correspond to the objects and distances that are within the FoV. Firstly, the analysis of the clustering detection and membership computation is highlighted for every test, and then the results comparison of several distance detection methods based on the information obtained from the clustering process is discussed.

Fig. 11a shows a representation of the first test, where an object has been placed between the distance detection system and a wall. Table 2 includes the distances measured by each of the 8 LIDAR segments. It is expected that the measurements of the middle segments would be grouped into a single cluster that corresponds to that of the object, and that there would be two other clusters that comprise the lateral measurements of the background. Fig. 12a depicts the initial membership matrix obtained during the test.

The membership matrix is composed of three clusters. The first two measurements, which are almost three meters away, would belong to the first cluster; the next five measurements, of more than two meters, to the second cluster of the object; and finally the last one that marks a distance similar to those of the first cluster belongs to the third cluster. Fig. 12b represents the matrix of belonging after the fuzzification process. Membership values have not changed significantly with respect to the initial matrix, which implies that the separation between the clusters is large enough that the degrees of belonging in the boundary measurements are not blurred.

Fig. 12a and 12b also shows the degree of belonging of each LIDAR segment measurement to each cluster for the results obtained in this first preliminary scenario (before and after fuzzy clustering, respectively).

A slightly different situation is shown in Fig. 11b for the second test. In this case there is still an object in the

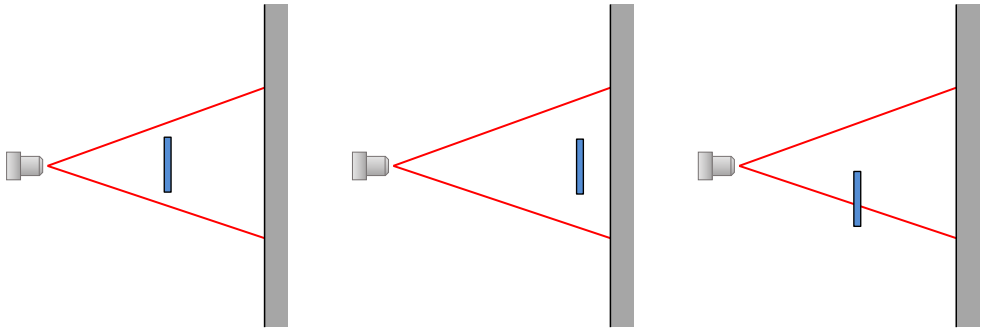

(a) Illustration of the LIDAR's FoV for the first test.

(b) Illustration of the LIDAR's FoV for the second test.

(c) Illustration of the LIDAR's FoV for the third test.

FIGURE 11. Representation of the scenario for tests 1, 2, and 3, showing the field of view of the LIDAR sensing system.

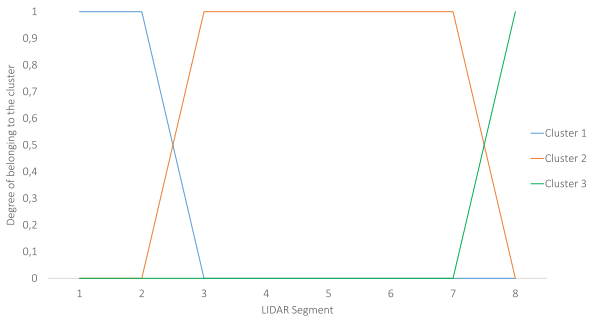

(a) Representation of the membership matrix for the obtained clusters.

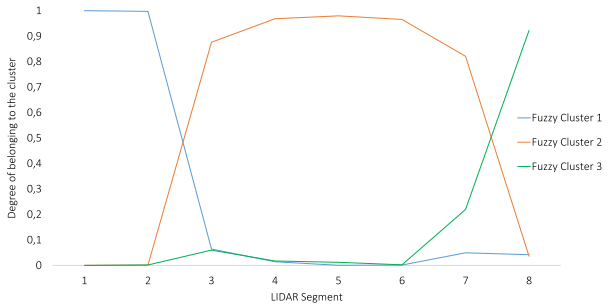

(b) Representation of the membership matrix for the obtained fuzzy clusters.

FIGURE 12. Representation of the membership matrices and the degree of belonging of each cluster for the preliminary test 1.

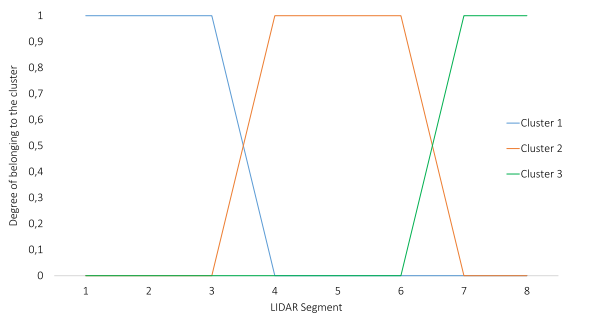

(a) Representation of the membership matrix for the obtained clusters.

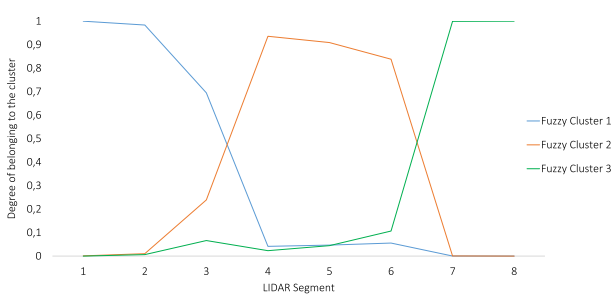

(b) Representation of the membership matrix for the obtained fuzzy clusters.

FIGURE 13. Representation of the membership matrices and the degree of belonging of each cluster for the preliminary test 2.

middle, but in a position much closer to the background wall. Table 2 contains the distances measured by each of the 8 LIDAR segments, while both the initial and fuzzification matrix are plotted in Fig. 13.

There are still three clusters, although as expected fewer segments detect the object since it is farther away from the LIDAR sensor, thus it occupies less space in the FoV. It can be seen that the degrees of belonging of the segment number five is more diffuse, since its measurement is the distance between the distance from the background and that of the object. This situation is better reflected with the fuzzification matrix outcomes, encountering it by the calculated degrees of belonging. Fig. 13a and 13b represents the degree of belonging of each LIDAR segment measurement to each cluster for the results obtained in this second test case (before and after fuzzy clustering, respectively).

In the third situation shown in Fig. 11c for this preliminary test, the object is partially introduced into the LIDAR's FoV. Table 2 contains the distances measured by each of the 8 LIDAR segments, while both the initial and fuzzification matrix for this case are shown in Fig. 14.

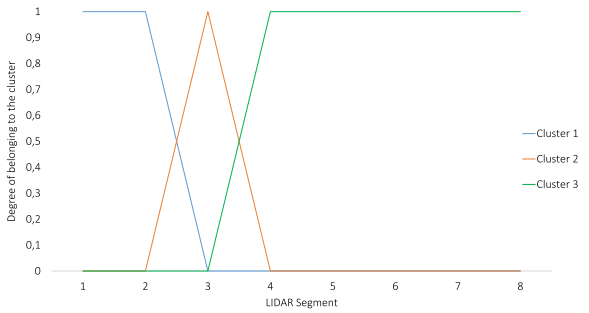

(a) Representation of the membership matrix for the obtained clusters.

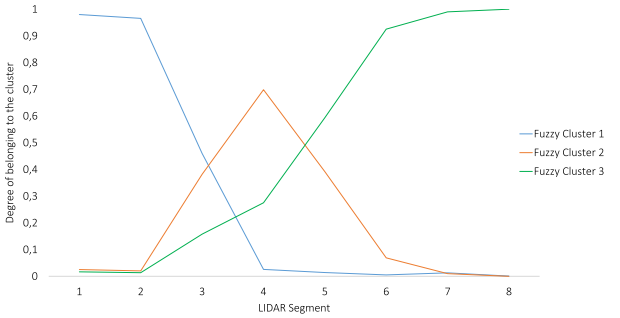

(b) Representation of the membership matrix for the obtained fuzzy clusters.

FIGURE 14. Representation of the membership matrices and the degree of belonging of each cluster for the preliminary test 3.

It can be seen a phenomenon that may not be infrequent. Segment 5 is measuring an intermediate distance between the distance of the first cluster and that of the last one, and therefore the clustering algorithm has assigned a specific cluster to it. This occurs when the object only covers a part of the angle of the field of view corresponding to the segment, and therefore the resulting distance will be an intermediate value between the two that coexist in that space. Thanks to the fuzzy clustering, the belonging of that segment that is giving a non-real measurements can be divided between the two adjacent clusters, which will make the final results closer to reality. Fig. 14a and 14b represents the degree of belonging of each LIDAR segment measurement to each cluster for the results obtained in this third test case (before and after fuzzy clustering, respectively).

Having a more adapted membership matrix based on the fuzzification process will ultimately allow calculating the target distance from the LIDAR sensor to the object of interest with higher accuracy, by applying the corresponding criteria, namely, a weighted mean function where the influence (i.e. the degree of belonging) of each segment within the cluster is considered to compute the distance; the average value in relationship with the membership of a segment in each cluster; a minimum value relative to the cluster detection; and a general average calculation in relationship with the overall segments. In order to compare these methods, Fig. 15 shows the results of the distance deviation with respect to the real

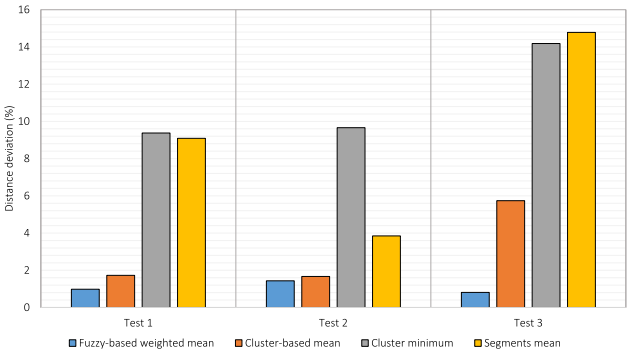

FIGURE 15. Comparison of the distance deviation results with respect to the actual distance of the sensing system to the object of interest.

distance to the object of interest, for the three test cases. It can be clearly seen the benefit of applying the fuzzy-based weighted function to obtain a value very close to the actual distance (which are 2.2, 2.6 and 2.3 meters for test 1, 2, and 3, respectively), achieving 0.9, 1.4 and 0.8 percent of error, respectively. It can be also highlighted that the variation between the first method and the rest of strategies is more predominant in situations where the fuzzy clustering and the calculation of the degree of belonging takes more significance, with a difference of almost 14% in accuracy in case of test 3. Therefore, the fuzzy-clustering based approach reports very-high accurate results for the distance detection in these situations with respect to the other methods.

B. RAILWAY USE CASE

The proposed system implementation has been verified in a real railway demonstrator scenario as part of the SCOTT project pilots [2], to measure and analyse the virtual coupling manoeuvres between trains under actual operational conditions. The distance measurement system based on the solid-state LIDAR sensor has been integrated within a heterogeneous Smart Train Composition Coupling platform, which also includes Vehicle-to-Vehicle communication and Wireless Sensor Networks for runtime virtual coupling and train integrity sensing tasks.

Apart from the integration of the proposed approach with the overall virtual coupling platform in terms of runtime sensing and data exchange, the project demonstrator allowed testing how the proposed distance detection system can be capable of providing information in compliant with the timing constraints requirements, and the consistency of the measurements with respect to the train manoeuvres under evaluation. The results of these verification objectives are the ones shown in this experimental use case section.

The location of the real demonstrator was a regular operation track for tourist purposes between Retz and Drosendorf, in Austria. The track has a total length of 40 km with a speed limit of 60 km/h. Two different trains have been used to carry out the tests. The first one was a six-wagon composition and the second one a rail coach, which are referred to as train A and train B, respectively. Pre-defined zones throughout

(a) Installation of the distance detection system in train A.

(b) Installation of the distance detection system in train B.

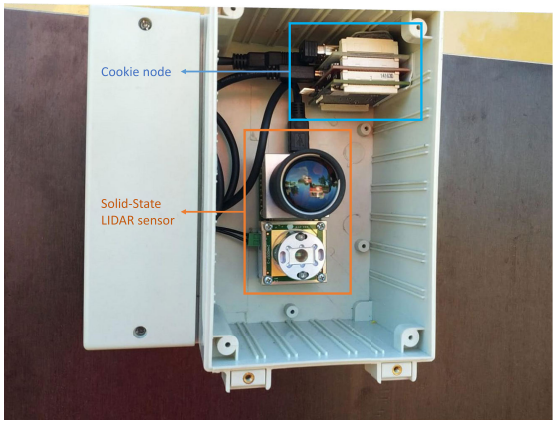

(c) Detailed view of the system installation, where the solid-state LIDAR sensor and the Cookie modular edge node integration is shown.

FIGURE 16. Implementation of the proposed distance detection system for virtual coupling in the target scenario, where the physical installation and location in both trains is highlighted.

the track have been used to perform the virtual coupling maneuver experiments.

In this way, the proposed system implementation has been deployed in both trains, as shown in Fig. 16. It can be seen the installation of the LIDAR sensors together with the modular wireless sensor nodes in an adapted mechanical box on rear and front platforms, respectively, to have a proper direct sight of the proximity detection zone. Initial experiments were carried with separation tests from 0 to 20 meters first and then from 20 to 100 meters, in slow movement conditions and measuring the actual distance, to firstly confirm the correct operation of the system in the real scenario prior to go the dynamic condition tests, obtaining consistency detections outcomes from the LIDAR sensing system with errors below 1 meter with respect to the actual separation distance.

Based on this configuration, different journeys for distance testing have been performed, distinguishing short distance approximation and detection, short-to-long range operation and detection, coupling distance and tracking between trains, and mix route operation with curves and long-range distance points detection on the field of view. The measurement campaign took place between the 6th and 10th of July 2020. During the dynamic operational conditions the results have been compared with the inferred V2V distance calculated from the geo-positioning of the trains in movement, provided by the WSN integrity sensing system installed on them. This value had a tolerance of ± 10 meters, which corresponds to a higher error than those obtained with the proposed system.

In the following representative tests the proximity detection has been properly verified based on the LIDAR sensing system, in which the distance processed and provisioned by the sensor node is consistent with the experimental scenario under test. Fig. 17 depicts the results for a virtual coupling scenario between train A and train B, where both trains are moving one after another with a separation distance varying between 10 and 14 m. This distance is detected by the sensor and represented in the plot. Trains were moving with a speed between 40 and 60 km/h. Fig. 17a also shows a picture of one of the instants during this virtual coupling test, taken from train A.

It can be seen in Fig. 17a the data associated with the processed LIDAR segments, which contains information of the field of view, so more objects apart from the fundamental distance can be acquired in the view. It can be realized that since the distance between both trains is reduced (almost the whole FoV corresponds to the object of interest), the dispersion of the different segments is also reduced, allowing a precised detection of the object based on the closest and central computed cluster. Based on the clustering and post-processing functions on the sensor node, the proximity detection is obtained, providing the results shown in Fig. 17b. The inferred distance curves are also represented in Fig. 17b to clearly see the tendency matching between the LIDAR based sensing and the localization based sensing. It can be also highlighted the stability of the measurements provided by the LIDAR sensing system.

The results in Fig. 18 show the test case where the distance detection between trains is obtained for a manoeuvre where there is a progressive separation between them. Both the distance segments detection from the LIDAR's field of view and the data processing outcomes are depicted to show how the LIDAR is capable of detecting different objects,

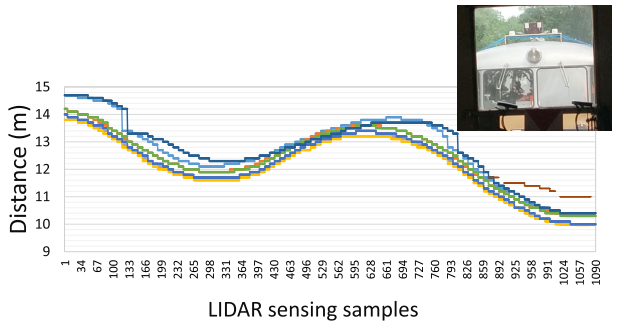

(a) Distance detection curve and photo of one of the instants of the proximity test between train A and train B, showing the separation between them.

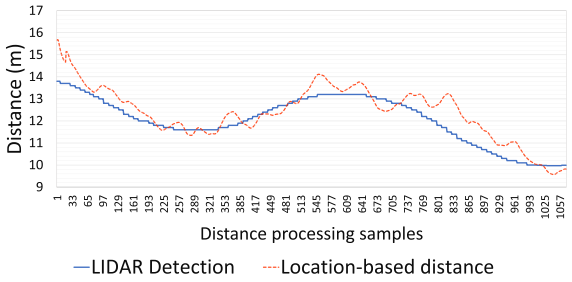

(b) Proximity distance processing outcomes, and its comparison with the location-based V2V inferred distance.

FIGURE 17. Distance detection results for the first virtual coupling test.

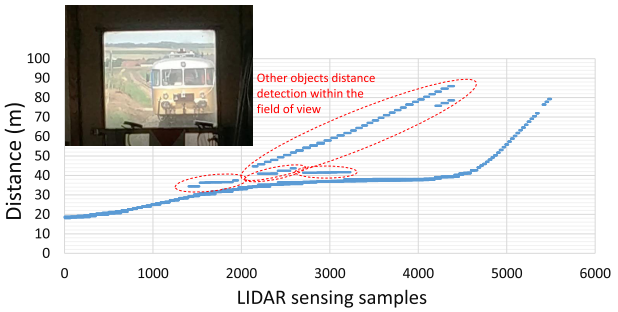

(a) Distance detection curve and photo of one of the instants of the proximity test between train A and train B, showing the separation between them.

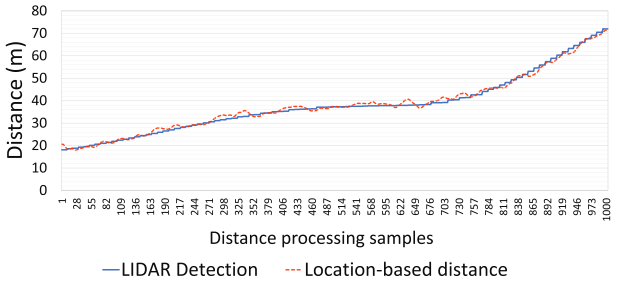

(b) Proximity distance processing outcomes, and its comparison with the location-based V2V inferred distance.

FIGURE 18. Distance detection results for the second virtual coupling test.

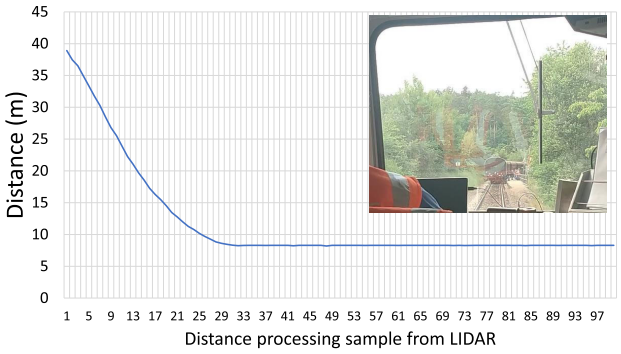

FIGURE 19. Distance processing results for the virtual coupling approaching manoeuvre, and photo of one of the instants of the proximity test between train A and train B.

and then the sensor node provides a filtered and processed data for the proximity information entity related to the object distance detection. As highlighted in Fig. 18a (which provides a unified sampling view of the distance segments), several object detections are concurrently performed, although the target separation distance between trains is properly obtained, as shown in the plot of Fig. 18b. The inferred distance curves are also represented in Fig. 18b to clearly see the tendency matching between the LIDAR based sensing and the localization based sensing. Detections go from 18 to 90 m in this experimental case. Fig. 18a also shows a picture of one of the instants during this proximity test, taken from train A.

Fig. 19 shows the test case of a proximity manoeuvre where trains are progressively getting closer to assess the operation of the approaching detection. The LIDAR based sensor nodes obtained and processed at runtime the distance measurements providing the detection data of the approaching curve represented in the plot, going from 39 meters (and approximately 16 km/h) to 8 m of separation between trains, with a gradual slowing speed during the approximation. It clearly shows how the processed information provides a consistent outcome for the distance detection. Fig. 19 also shows a picture of one of the instants during the above-described approaching manoeuvre between both trains, taken from train B.

Table 3 shows the comparison of the parameters that have been considered as the target requirements for the testing scenario, and the implementation outcomes of the proposed distance detection solution, obtaining 63.8% of reduction in terms of response time, and one order or magnitude of higher accuracy with respect to the minimum required distance precision, for the distance detection range of 100 meters. Moreover, the system has been able to properly detect distances up to 120 meters, which is a 20% higher than the requested maximum value for the use case scenario.

TABLE 3. Parameters' requirements versus implementation outcomes for the use case scenario.

Parameter	Scenario requirements	Test results
Response time	500 ms	0.185 ms (max.)
Distance error	< 10 m	< 1 m
Distance detection range	100 m	120 m

C. FURTHER OPERATING CONSIDERATIONS

The measurement campaigns and the experimental outcomes allowed verifying the proposed sensing system under a real railway context and its feasibility to be integrated in the overall railway smart train paradigm. From the point of view of the ultimate deployment of the sensing system within long-term commercial railway operation, there are several additional considerations to cope with. Although the LIDAR sensors may have a degradation in the measurement in some environmental conditions, it is not as pronounced as in case of cameras, where the object detections are prone to have a significant loss in accuracy, readability and feasibility of the processing outcomes. The railway operators and integrators involved in this type of use case have been interested in integrating and fusioning different technologies and particularly the LIDAR sensing approach to provide robust and safety conditions where the virtual coupling maneuvers between trains can be performed. In this regard, three levels of safety conditions are distinguished to dynamically decide whether the maneuver can be carried out or, instead, the integrity and virtual coupling mission has to be aborted, in accordance with the different levels of redundancy provided by the overall Smart Train Composition Coupling architecture.

First, since the LIDAR sensing system is deployed in both trains, the segment detections as well as the fuzzy clustering outcomes are distributed between them to dynamically compare if the mismatches in terms of distance detections to the object of interest are above a safety threshold (for instance, in the case of adverse weather conditions). If so, the LIDAR based detection would not be used during the redundancy verification process of the virtual coupling conditions. Then, even if the threshold is not exceeded, a second redundancy stage is performed to guarantee that both independent LIDAR measurements are not corrupted. This second level relies on the V2V radio measurements that allow inferring the distance through the wireless communication between the adjacent trains, and this is also combined with the inference of the relative distance between them calculated from the geo-positioning information provided by the Wireless Sensor Network. These parameters are interchanged between the two sensing systems, so that if the verification between the three independent sources of measurement produces a mismatch value above a safety threshold the mission is not triggered or is ended.

The third consideration to guarantee that a virtual coupling operation can be safely carried out is based on the definition of zones in the railway track for accomplishing the maneuvers, as well as meeting specific conditions of train operations that may also include the possibility to restrict them for safety reasons due to external factors (such as weather hazards or a probability of occurring possible damaging situations). Therefore, in case the measurement is compromised for internal or external reasons, the redundancy stages and the operating conditions will also take place to decide whether the virtual coupling can be carried out.

V. CONCLUSION AND FUTURE WORK

The implementation, integration, and testing of the solid-state LIDAR sensor wiith the modular Cookie edge sensor platform and the results regarding the presented experimental railway demonstrator allowed showing the potential of the proposed distance measurement and detection system to serve as a dual redundancy solution, which shall be combined with V2V wireless communication between trains to provide accurate and safety solutions towards railway virtual coupling. Although the preliminary railway tests correspond to a system verification stage, they provide a contextualized vision of solid-state based LIDAR sensing system, obtaining consistent results to be further explored in future implementations and exploitation of the virtual coupling solution. As future lines of work, it is envisioned to carry out further measurement campaigns in middle-speed controlled railway pilots, to test additional reliability and safety conditions. In this direction, automatic virtual coupling and uncoupling manoeuvre tests will allow analysing the combination of the distance detection system and the V2V communication technology to assure timing and accuracy compliance in such a next constrained level.

ACKNOWLEDGMENT

The SCOTT project received funding from the ECSEL Joint Undetaking with the support of the European Union's Horizon 2020 research and innovation programme and several countries such as Austria, Spain, Finland, Ireland, Sweden, Germany, Poland, Portugal, Netherlands, Belgium and Norway.

REFERENCES

[1] Shift2Rail Joint Undertaking. *European Commission Initiative to Promote the Research and Innovation in the European Railway Domain*. Accessed: Mar. 2, 2021. [Online]. Available: https://shift2rail.org/about-shift2rail/mission-and-objectives/

[2] SCOTT. *Secure, COnnected Trustable Things, Ecsel Joint Undertaking European Project*. Accessed: Mar. 2, 2021. [Online]. Available: https://scottproject.eu/

[3] European Union Agency for Railways. *ERTMS Operational Principles and Rules. Technical Document*. Accessed: Mar. 2, 2021. [Online]. Available: https://www.era.europa.eu/sites/default/files/activities/docs/appendix_a_ope_tsi_v5_en.pdf

[4] F. Flammini, S. Marrone, R. Nardone, A. Petrillo, S. Santini, and V. Vittorini, "Towards railway virtual coupling," in *Proc. IEEE Int. Conf. Electr. Syst. Aircr., Railway, Ship Propuls. Road Vehicles Int. Transp. Electrific. Conf. (ESARS-ITEC)*, Nov. 2018, pp. 1–6.

[5] X. Wang, L. Liu, L. Zhu, and T. Tang, "Train-centric CBTC meets age of information in train-to-train communications," *IEEE Trans. Intell. Transp. Syst.*, vol. 21, no. 10, pp. 4072–4085, Oct. 2020.

[6] J. Portilla, G. Mujica, J.-S. Lee, and T. Riesgo, "The extreme edge at the bottom of the Internet of Things: A review," *IEEE Sensors J.*, vol. 19, no. 9, pp. 3179–3190, May 2019.

[7] J. Lichtblau, B. Scheiner, F. Michler, M. Graebner, B. Sanftl, R. Weigel, and A. Koelpin, "Novel approach for virtual coupling of trains using different modulation and coding schemes," in *Proc. Int. Conf. Intell. Rail Transp. (ICIRT)*, Dec. 2018, pp. 1–4.

[8] T. Ye, X. Zhang, Y. Zhang, and J. Liu, "Railway traffic object detection using differential feature fusion convolution neural network," *IEEE Trans. Intell. Transp. Syst.*, vol. 22, no. 3, pp. 1375–1387, Mar. 2021.

[9] K. Takagi, K. Morikawa, T. Ogawa, and M. Saburi, "Road environment recognition using on-vehicle LIDAR," in *Proc. IEEE Intell. Vehicles Symp.*, Jun. 2006, pp. 120–125.

[10] D. Z. Wang, I. Posner, and P. Newman, "Model-free detection and tracking of dynamic objects with 2D lidar," *Int. J. Robot. Res.*, vol. 34, no. 7, pp. 1039–1063, Jun. 2015.

[11] C. Mertz, L. E. Navarro-Serment, R. MacLachlan, P. Rybski, A. Steinfeld, A. Suppé, C. Urmson, N. Vandapel, M. Hebert, C. Thorpe, D. Duggins, and J. Gowdy, "Moving object detection with laser scanners," *J. Field Robot.*, vol. 30, no. 1, pp. 17–43, Jan. 2013.
[12] B. Qin, Z. J. Chong, S. H. Soh, T. Bandyopadhyay, M. H. Ang, E. Frazzoli, and D. Rus, "A spatial-temporal approach for moving object recognition with 2d lidar," in *Experimental Robotics*. Cham, Switzerland: Springer, 2016, pp. 807–820.
[13] N. Corso and A. Zakhor, "Indoor localization algorithms for an ambulatory human operated 3D mobile mapping system," *Remote Sens.*, vol. 5, no. 12, pp. 6611–6646, Dec. 2013.
[14] J. A. Hesch, F. M. Mirzaei, G. L. Mariottini, and S. I. Roumeliotis, "A laser-aided inertial navigation system (L-INS) for human localization in unknown indoor environments," in *Proc. IEEE Int. Conf. Robot. Autom.*, May 2010, pp. 5376–5382.
[15] E. J. Means, A. S. Acker, J. D. Harding, J. B. Blair, A. M. Lefsky, B. W. Cohen, E. M. Harmon, and W. A. McKee, "Use of large-footprint scanning airborne lidar to estimate forest stand characteristics in the western cascades of Oregon," *Remote Sens. Environ.*, vol. 67, no. 3, pp. 298–308, Mar. 1999.
[16] A. Jaakkola, "Low-cost mobile laser scanning and its feasibility for environmental mapping," Ph.D. dissertation, Aalto Univ., Espoo, Finland, 2015.
[17] R. Zlot and M. Bosse, "Three-dimensional mobile mapping of caves," *J. Cave Karst Stud.*, vol. 76, no. 3, pp. 191–206, Dec. 2014.
[18] C. Hopkinson, L. Chasmer, C. Young-Pow, and P. Treitz, "Assessing forest metrics with a ground-based scanning lidar," *Can. J. Forest Res.*, vol. 34, no. 3, pp. 573–583, Mar. 2004.
[19] A. Yilmaz, O. Javed, and M. Shah, "Object tracking: A survey," *ACM Comput. Surv.*, vol. 38, no. 4, p. 13, 2006.
[20] K. O. Arras, O. M. Mozos, and W. Burgard, "Using boosted features for the detection of people in 2D range data," in *Proc. IEEE Int. Conf. Robot. Autom.*, Apr. 2007, pp. 3402–3407.
[21] T.-D. Vu and O. Aycard, "Laser-based detection and tracking moving objects using data-driven Markov chain Monte Carlo," in *Proc. IEEE Int. Conf. Robot. Autom.*, May 2009, pp. 3800–3806.
[22] V. Vaquero, E. Repiso, and A. Sanfeliu, "Robust and real-time detection and tracking of moving objects with minimum 2D LiDAR information to advance autonomous cargo handling in ports," *Sensors*, vol. 19, no. 1, p. 107, Dec. 2018.
[23] T. Miyasaka, Y. Ohama, and Y. Ninomiya, "Ego-motion estimation and moving object tracking using multi-layer LIDAR," in *Proc. IEEE Intell. Vehicles Symp.*, Jun. 2009, pp. 151–156.
[24] E. Arnold, O. Y. Al-Jarrah, M. Dianati, S. Fallah, D. Oxtoby, and A. Mouzakitis, "A survey on 3D object detection methods for autonomous driving applications," *IEEE Trans. Intell. Transp. Syst.*, vol. 20, no. 10, pp. 3782–3795, Oct. 2019.
[25] S. U. Sharma and D. J. Shah, "A practical animal detection and collision avoidance system using computer vision technique," *IEEE Access*, vol. 5, pp. 347–358, 2017.
[26] Y. Bai and D. Wang, "Fundamentals of fuzzy logic control—Fuzzy sets, fuzzy rules and defuzzifications," in *Advanced Fuzzy Logic Technologies in Industrial Applications*. London, U.K.: Springer, 2006, pp. 17–36.
[27] J. C. Bezdek, *Pattern Recognition With Fuzzy Objective Function Algorithms* (Advanced Applications in Pattern Recognition Series). New York, NY, USA: Springer, 2013.
[28] X. Zhang, W. Pan, Z. Wu, J. Chen, Y. Mao, and R. Wu, "Robust image segmentation using fuzzy C-means clustering with spatial information based on total generalized variation," *IEEE Access*, vol. 8, pp. 95681–95697, 2020.
[29] K.-S. Chuang, H.-L. Tzeng, S. Chen, J. Wu, and T.-J. Chen, "Fuzzy C-means clustering with spatial information for image segmentation," *Comput. Med. Imag. Graph.*, vol. 30, no. 1, pp. 9–15, Jan. 2006.
[30] M.-S. Yang, Y.-J. Hu, K. C.-R. Lin, and C. C.-L. Lin, "Segmentation techniques for tissue differentiation in MRI of ophthalmology using fuzzy clustering algorithms," *Magn. Reson. Imag.*, vol. 20, no. 2, pp. 173–179, Feb. 2002.
[31] Y. Zhang, C. Ma, Y. Wang, S. Zhang, and P. Wan, "Information geometry-based fuzzy-C means algorithm for cooperative spectrum sensing," *IEEE Access*, vol. 8, pp. 155742–155752, 2020.
[32] C.-H. Yang, L.-Y. Chuang, and Y.-D. Lin, "Epistasis analysis using an improved fuzzy C-means-based entropy approach," *IEEE Trans. Fuzzy Syst.*, vol. 28, no. 4, pp. 718–730, Apr. 2020.
[33] C. Wang, W. Pedrycz, J. Yang, M. Zhou, and Z. Li, "Wavelet frame-based fuzzy C-means clustering for segmenting images on graphs," *IEEE Trans. Cybern.*, vol. 50, no. 9, pp. 3938–3949, Sep. 2020.
[34] LeddarTech. *Leddar Vu8, 8-Segment Solid-State LIDAR Sensor*. Accessed: Mar. 2, 2021. [Online]. Available: https://leddartech.com/solutions/leddar-vu8-solid-state-lidar-sensor-module/
[35] J. Portilla, A. de Castro, E. de la Torre, and T. Riesgo, "A modular architecture for nodes in wireless sensor networks," *J. Universal Comput. Sci.*, vol. 12, no. 3, pp. 328–339, 2006.
[36] P. Merino, G. Mujica, J. Señor, and J. Portilla, "A modular IoT hardware platform for distributed and secured extreme edge computing," *Electronics*, vol. 9, no. 3, p. 538, Mar. 2020.
[37] Microchip. *SAMA5D3 Series, a High-Performance, Ultra-Low-Power ARM Cortex-A5 Processor-Based MPU*. Accessed: Mar. 2, 2021. [Online]. Available: https://www.microchip.com/wwwproducts/en/ATsama5d36

GABRIEL MUJICA (Member, IEEE) received the Ph.D. degree in industrial electronics engineering from the Universidad Politécnica de Madrid (UPM).

He is currently an Assistant Professor and a Research Member with the Center of Industrial Electronics, UPM, where he is mainly involved in the area of the Internet of Things, networked embedded systems, and wireless sensor networks (WSNs). He has participated in different national and European research projects (including Horizon 2020 projects), related to the development and optimization of WSN, as well as the integration of heterogeneous IoT edge hardware, software, and communication technologies for wireless distributed systems, with a particular focus on the performance evaluation and optimization of sensor platforms under real deployment contexts. He has authored several contributions in high-impact conferences and journals. He has collaborated in the organization of research tutorials and seminars, and as a reviewer and a guest editor in international conferences and indexed journals. Moreover, his visiting research stay at the Trinity College Dublin strengthened the vision and applicability of the IoT technologies for smart and sustainable cities, leveraging collaborations in the area of distributed systems within such contexts. His current research interests include multi-hop distributed networks, hardware-software co-design, and protocols for the IoT embedded systems in smart urban application scenarios.

JAVIER HENCHE received the B.S. and M.Sc. degrees in industrial electronics engineering from the Universidad Politécnica de Madrid (UPM), in 2018 and 2020, respectively, He currently collaborated in research projects at the Center of Industrial Electronics, UPM, related to the characterisation, application, and testing of LIDAR technologies for the railway domain. His research interests include hardware and software integration for the IoT edge sensing and wireless sensor networks embedded platforms.

JORGE PORTILLA (Senior Member, IEEE) received the M.Sc. degree in physics from the Universidad Complutense de Madrid, Madrid, Spain, in 2003, and the Ph.D. degree in electronic engineering from the Universidad Politécnica de Madrid (UPM), Madrid, in 2010.

He was a Visiting Researcher with the Industrial Technology Research Institute, Hsinchu, Taiwan, in 2008, and with the National Taipei University of Technology (Taipei Tech), Taipei, Taiwan, in 2018, working on wireless sensor networks hardware platforms and network clustering techniques. He is currently an Associate Professor with UPM. He carries out his research activity within the Centro de Electrónica Industrial, belonging to the UPM. He has participated in more than 30 funded research projects, including European Union FP7 and H2020 projects, and Spain Government funded projects, as well as private industry funded projects, mainly related to wireless sensor networks and the Internet of Things. He has numerous publications in prestigious international conferences as well as in journals with impact factor. His research interests include wireless sensor networks, the Internet of Things, digital embedded systems, and reconfigurable FPGA-based embedded systems.